CHIN. PHYS. LETT. Vol. 34, No. 6 (2017) 060202

A High-Order Conservative Numerical Method for Gross–Pitaevskii Equation with Time-Varying Coefficients in Modeling BEC *

Xiang Li(李翔)[1], Xu Qian(钱旭)[1,2**], Ling-Yan Tang(唐玲艳)[1], Song-He Song(宋松和)[1]

[1]*College of Science and State Key Laboratory of High Performance Computing, National University of Defense Technology, Changsha 410073*

[2]*Academy of Ocean Science and Engineering, National University of Defense Technology, Changsha 410073*

(Received 5 January 2017)

We propose a high-order conservative method for the nonlinear Schrödinger/Gross–Pitaevskii equation with time-varying coefficients in modeling Bose–Einstein condensation (BEC). This scheme combined with the sixth-order compact finite difference method and the fourth-order average vector field method, finely describes the condensate wave function and physical characteristics in some small potential wells. Numerical experiments are presented to demonstrate that our numerical scheme is efficient by the comparison with the Fourier pseudo-spectral method. Moreover, it preserves several conservation laws well and even exactly under some specific conditions.

PACS: 02.60.Lj, 02.70.Bf, 02.60.Cb, 02.60.Jh

DOI: 10.1088/0256-307X/34/6/060202

Many well-known nonlinear Schrödinger equations are widely used to describe physical phenomena, such as nonlinear optics, plasma physics and many practical problems in quantum physics, especially for the study of Bose–Einstein condensation (BEC) at extremely low temperature, which is also called the Gross–Pitaevskii (GP) equation.[1,2] This real physical equation customarily possesses variable coefficients, which are mainly used to study the collective behavior of macroscopic ensemble of Bose-particles occupying the same ground state. The condensate typically contains millions of atoms that would be confined in magnetic traps and cooled down to extremely low temperatures. Hence, experimental achievements in confining the BEC by a trap potential may relieve the restrictions of temperature. Therefore, a variety of spacial potential functions have been proposed for BEC.[3]

We begin by introducing the $n+1$ model Schrödinger equation with a time-independent external potential, which reads

$$i\hbar\Psi_t = \Big(-\frac{\hbar^2}{2m}\nabla^2 + g|\Psi|^2 + \epsilon X(\boldsymbol{r})\Big)\Psi.$$

Considering the following GP equation (1+1 model) with time-varying coefficients in a small trapped potential,

$$i\Psi_t = -(\alpha(t)\nabla^2 + \gamma(t)|\Psi|^2 + \beta(t)X(x))\Psi, \quad (1)$$

we proceed defining $\Psi(x,t)$ to be a complex-valued wave function, where $(x,t)\in[-L,L]\times\mathbb{R}^+$, with the initial condition

$$\Psi(x,0) = \varphi(x),\ x\in[-L,L],$$

and the boundary condition $\Psi(-L,t) = \Psi(L,t)$. These bounded real functions, $\alpha(t)$, $\gamma(t)$ and $\beta(t)$, are all time-dependent coefficients. In particular, $\alpha(t)$ and $\gamma(t)$ are related to the atom scattering length, where $\gamma>0$ ($\gamma<0$) is expected for the attractive or focusing interaction (the repulsive or defocusing interaction), $X(x)$ is given as the trap potential, and usually can be chosen for the harmonic trap potential or the periodic collapse potential, and $\beta(t)$ denotes the assumed coefficient of time.

For the initial value problem, Eq. (1) satisfies two conserved quantities,[4] as follows: (1) charge conservation law

$$Q(\Psi) = \int_R |\Psi|^2 dx = Q(\varphi), \quad (2)$$

and (2) energy conservation law, if $\alpha(t)$, $\gamma(t)$ and $\beta(t)$ are independent of t (i.e., $\alpha(t)=\alpha_0$, $\gamma(t)=\gamma_0$, $\beta(t)=\beta_0$), then

$$\begin{aligned} E(\Psi) &= \int_R \Big(\alpha|\Psi_x|^2 - \beta X(x)|\Psi|^2 - \frac{1}{2}\gamma|\Psi|^4\Big)dx \\ &= \int_R \Big(\alpha_0|\Psi_x|^2 - \beta_0 X(x)|\Psi|^2 - \frac{1}{2}\gamma_0|\Psi|^4\Big)dx \\ &= E(\varphi). \end{aligned} \quad (3)$$

Since the available theoretical methods for the GP equation are unable to meet harsh requirements in practical issues, the numerical approach is an important tool to understand the physical behavior of this model. Accordingly, Bao and Shen proposed a time-splitting Laguerre–Hermite pseudo-spectral method.[5] Mehdi and Ameneh used the compact split-step finite difference method to solve the GP system with constant and variable coefficients.[6] Kong and Hong provided a symplectic geometric algorithm for the GP equation in high dimensions,[4] which possesses long-time computing advantages. On the one hand, considering the importance of the trap

*Supported by the National Natural Science Foundation of China under Grant Nos 11571366 and 11501570, the Open Foundation of State Key Laboratory of High Performance Computing of China, the Research Fund of National University of Defense Technology under Grant No JC15-02-02, and the Fund from HPCL.

**Corresponding author. Email: qianxu@nudt.edu.cn

© 2017 Chinese Physical Society and IOP Publishing Ltd

potential, the stationary solutions of BEC in different potentials were discussed. For example, there are ring-shaped potentials,[7] double-well potentials[8] and multi-well potentials.[9] On the other hand, the homogeneous principle, the F-expansions technique and the Jacobi elliptic functions are widely used to construct the bright solutions (BSs) or dark solutions (DSs) of BEC.[10–14]

Letting $\Psi = u + iv$, Eq. (1) can be expressed in the finite-dimensional Hamiltonian form

$$\frac{d\boldsymbol{z}}{dt} = J^{-1}\frac{\delta H}{\delta \boldsymbol{z}}, \quad J^{-1} = \begin{pmatrix} 0 & 1 \\ -1 & 0 \end{pmatrix}, \tag{4}$$

where $\boldsymbol{z} = [u, v]^{\mathrm{T}}$, the Hamiltonian function of Eq. (1) is

$$H(\boldsymbol{z}) = \int_R (\alpha((u_x)^2 + (v_x)^2) - \beta X(x)(u^2 + v^2) - \frac{\gamma}{2}(u^2 + v^2)^2)dx. \tag{5}$$

By applying the sixth-order compact finite difference method (CFDM) in the space direction,[15] we firstly discretize the spatial-temporal region $[-L, L] \times [0, T]$ with coordinates $x_j = (j \times h - L)$, $j = 0, 1, \ldots, N$ and $t_n = n \times \tau$, $n = 0, 1, \ldots, \hat{N}$, where $h = 2L/N$ and $\tau = T/\hat{N}$ are the spatial step length and the temporal step length, respectively. To ensure the scheme to be non-dissipative, we set the stencil-state and the weighted factors to be symmetric. Therefore, the stated formula for the first-order derivative $(\Psi_x)_j$ is

$$\sigma(\Psi_x)_{j-1} + (\Psi_x)_j + \sigma(\Psi_x)_{j+1} = \lambda\frac{\Psi_{j+2} - \Psi_{j-2}}{4h} + \omega\frac{\Psi_{j+1} - \Psi_{j-1}}{2h}.$$

Because the theoretical precision depends upon selection of these unknown coefficients, we designate the sixth-order restrictive selection condition as follows:

$$\omega + 2^4\lambda = 10\sigma.$$

Choosing σ as the free parameter, we derive a set of schemes $\omega = 2/3(\sigma + 2)$, $\lambda = 1/3(4\sigma - 1)$. Furthermore, we derive a sixth-order approximation with $\sigma = \frac{1}{3}$, $\omega = \frac{14}{9}$, $\lambda = \frac{1}{9}$, and the major truncation error is $\frac{4}{7!}\Psi^{(7)}h^6$. Under the appropriate periodic or homogeneous boundary condition, the discrete approximation can be written as the following matrix form

$$\boldsymbol{L}\hat{\Psi}_x = \boldsymbol{R}\hat{\Psi} \Longrightarrow \hat{\Psi}_x = \boldsymbol{D}\hat{\Psi}, \tag{6}$$

where $\hat{\Psi} = (\Psi_1, \Psi_2, \ldots, \Psi_j, \ldots, \Psi_N)$, $\boldsymbol{D} = \boldsymbol{L}^{-1}\boldsymbol{R}$, and

$$\boldsymbol{L} = \frac{1}{3}\begin{pmatrix} 3 & 1 & 0 & \ldots & 0 & 1 \\ 1 & 3 & 1 & \ldots & 0 & 0 \\ & & \ddots & \ddots & \ddots & \\ 0 & 0 & \ldots & 1 & 3 & 1 \\ 1 & 0 & \ldots & 0 & 1 & 3 \end{pmatrix},$$

$$\boldsymbol{R} = \frac{1}{36h}\begin{pmatrix} 0 & 28 & 1 & 0 & 0\ldots & 0 & -1 & -28 \\ -28 & 0 & 28 & 1 & 0\ldots & 0 & 0 & -1 \\ -1 & -28 & 0 & 28 & 1\ldots & 0 & 0 & 0 \\ & & \ddots & \ddots & \ddots & \ddots & \ddots & \\ 0 & 0 & 0\ldots & -1 & -28 & 0 & 28 & 1 \\ 1 & 0 & 0\ldots & 0 & -1 & -28 & 0 & 28 \\ 28 & 1 & 0\ldots & 0 & 0 & -1 & -28 & 0 \end{pmatrix}.$$

Obviously, $\boldsymbol{L}$ is real symmetric, and $\boldsymbol{R}$ is real skew-symmetric. The approximation to Ψ_{xx} can be written as $\hat{\Psi}_{xx} = \boldsymbol{D}_2\hat{\Psi}$, where $\boldsymbol{D}_2 = \boldsymbol{D}^2$ is also a real-symmetric matrix. For the theoretical analysis of non-dissipative and discrete conservation laws, we can refer to Ref. [15]. Moreover, the Fourier pseudo-spectral method (FPSM) with high accuracy has been verified in many applications.[16,17] Thus we take it as comparison. To be specific, we approximate the first-order spatial derivative by the Fourier pseudo-spectral matrix, which yields

$$(\boldsymbol{D}_F)_{j,l} = \begin{cases} \frac{1}{2}(-1)^{j+l}\eta\cot(\eta\frac{x_j - x_l}{2}), & j \neq l, \\ -\eta^2\frac{N^2+2}{12}, & j = l, \end{cases}$$

where $\eta = \frac{2\pi}{N}$.

The corresponding semi-discrete system of the compact difference method is

$$\begin{aligned}(u_t)_j =& -\alpha(t)(\boldsymbol{D}_2V)_j - \gamma(t)(u_j^2 + v_j^2)v \\ & - \beta(t)X(x)v_j, \\ (v_t)_j =& \alpha(t)(\boldsymbol{D}_2U)_j + \gamma(t)(u_j^2 + v_j^2)u \\ & + \beta(t)X(x)u_j. \end{aligned} \tag{7}$$

Similarly, Eq. (1) can also be expressed in the finite-dimensional Hamiltonian form

$$\frac{d\boldsymbol{z}}{dt} = \boldsymbol{J}^{-1}\nabla H(Z), \boldsymbol{J}^{-1} = \begin{pmatrix} 0 & I_N \\ -I_N & 0 \end{pmatrix}, \tag{8}$$

where $Z = [U, V]^{\mathrm{T}}$, I_N is an $N \times N$ unitary matrix, $U = (u_1, u_2, \ldots, u_N)$, and $V = (v_1, v_2, \ldots, v_N)$.

Based on the B-series of Hamiltonian vector field, Quispel and McLaren proposed the average vector field method (AVFM),[18] which would achieve high precision in time direction and would preserve the Hamiltonian exactly. Celledoni *et al.*[19] and other researchers[20–22] applied this method to various types of equations and achieved good results. Then, applying the fourth-order time-accurate AVFM[18] for Eq. (7) yields

$$\frac{z_j^{n+1} - z_j^n}{\tau} = (\delta_i^j - \frac{\tau^2}{12}f_k^j(\hat{z})f_i^k(\hat{z})) \cdot \int_0^1 f^i(\xi z^{n+1} + (1-\xi)z^n)d\xi. \tag{9}$$

Combining Eqs. (5) and (7) gives the following scheme

$$\frac{Z^{n+1} - Z^n}{\tau} = \begin{pmatrix} F^1 \\ F^2 \end{pmatrix} - \frac{\tau^2}{12}\begin{pmatrix} f_u^1(\hat{Z}) & f_v^1(\hat{Z}) \\ f_u^2(\hat{Z}) & f_v^2(\hat{Z}) \end{pmatrix} \cdot \begin{pmatrix} f_u^1(\hat{Z}) & f_v^1(\hat{Z}) \\ f_u^2(\hat{Z}) & f_v^2(\hat{Z}) \end{pmatrix}\begin{pmatrix} F^1 \\ F^2 \end{pmatrix}, \tag{10}$$

where $F^i = \int_0^1 f^i(\xi z^{n+1} + (1-\xi)z^n)d\xi$. According to the accuracy condition of AVFM,[18] we choose the following average stencil

$$\hat{u} = \frac{1}{2}(u^{n+1} + u^n),\ \hat{v} = \frac{1}{2}(v^{n+1} + v^n),$$
$$\hat{\alpha} = \frac{1}{2}(\alpha^{n+1} + \alpha^n),\ \hat{\gamma} = \frac{1}{2}(\gamma^{n+1} + \gamma^n),$$
$$\hat{\beta} = \frac{1}{2}(\beta^{n+1} + \beta^n).$$

If take α as an example, we will have

$$\alpha^{n+1} = \alpha((n+1)\times\tau),\ \alpha^n = \alpha(n\times\tau).$$

Next, as for dealing with F^i in Eq. (10), we use the following approximations

$$\begin{aligned}
F_j^1 &= (F_j^1)_1 + (F_j^1)_2 + (F_j^1)_3,\\
(F_j^1)_1 &= -\int_0^1 (\xi\alpha^{n+1} + (1-\xi)\alpha^n)(\boldsymbol{D}_2(\xi V^{n+1}\\
&\quad + (1-\xi)V^n))_j d\xi,\\
(F_j^1)_2 &= -\int_0^1 (\xi\gamma^{n+1} + (1-\xi)\gamma^n)(\xi v_j^{n+1}\\
&\quad + (1-\xi)v_j^n)[(\xi u_j^{n+1} + (1-\xi)u_j^n)^2\\
&\quad + (\xi v_j^{n+1} + (1-\xi)v_j^n)^2]d\xi,\\
(F_j^1)_3 &= -X(x_j)\int_0^1 (\xi\beta^{n+1} + (1-\xi)\beta^n)(\xi v_j^{n+1}\\
&\quad + (1-\xi)v_j^n)d\xi.
\end{aligned}$$

To deal with the time-varying coefficients in BECs, we apply the classical AVFM for calculating F^1 and F^2. After that, we can obtain the linear combination of these coefficients, which could be easily solved.

Thus the full discrete form of Eq. (10) can be written approximately as

$$\begin{pmatrix} \frac{U^{n+1}-U^n}{\tau} \\ \frac{V^{n+1}-V^n}{\tau} \end{pmatrix} = \begin{pmatrix} F^1 \\ F^2 \end{pmatrix} - \begin{pmatrix} \Delta_{11} & \Delta_{12} \\ \Delta_{21} & \Delta_{22} \end{pmatrix} \begin{pmatrix} F^1 \\ F^2 \end{pmatrix}, \quad (11)$$

and we take the following discrete Hamiltonian

$$\begin{aligned}
H_E^n = \sum_{j=1}^{N} \Big[&\alpha^n(((\boldsymbol{D}_2U)_j)^2 + ((\boldsymbol{D}_2V)_j)^2)\\
&- \beta^n X(x_j)(u_j^2 + v_j^2) - \frac{1}{2}\gamma^n(u_j^2 + v_j^2)^2\Big]. \quad (12)
\end{aligned}$$

Then, we turn our attention toward the four classic physical waveform examples to verify the efficiency of the proposed scheme for the GP equation. For example 1, we set the periodic collapse potential, which is also called the lattice trap and where $X = \cos^2(x)$. It is useful to study the one-dimensional dynamics of cold atoms BEC in parabolic optical lattices. When taking the coefficients as $\alpha = \frac{1}{2}$, $\gamma = -1$ and $\beta = -1$, Eq. (1) has its analytical solution $\Psi_e(x,t) = \exp(-\frac{it}{2})\sin(x)$. Under the initial condition $\varphi(x) = \sin(x)$, we notice that Fig. 1 displays the propagation of the multi-solitary wave and the periodic collapse of amplitude. In contrast, the numerical collapse wave intensity $|\Psi|^2$ agrees very well with its analytical solution till $t = 50$ s. It can be obtained from Table 1 that the proposed scheme can achieve high accuracy numerically the same as FPSM.

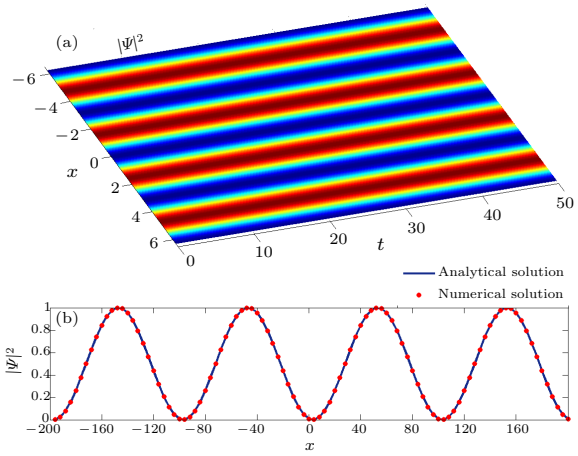

Fig. 1. (a) Multi-solitary waves with the periodic collapse potential on four-period interval ($L = 2\pi$, $N = 400$ and $dt = 0.005$) and (b) the comparison between analytical and numerical solutions at $t = 50$ s. Here x in (a) and (b) are different scales.

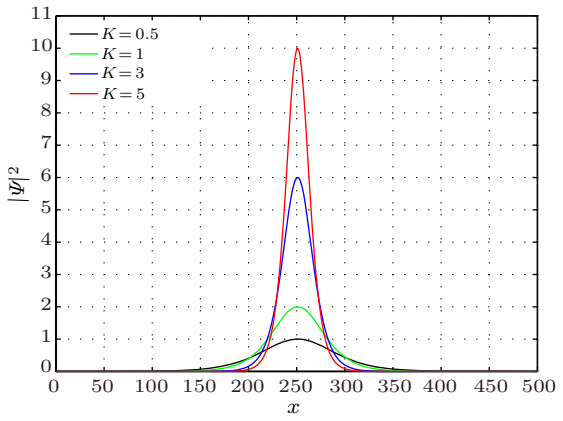

Fig. 2. The steady-state soliton solution at $t = 10$ s under specially selected K ($X = \frac{1}{2}x^2$, $L = 5$, $N = 500$ and $dt = 0.01$).

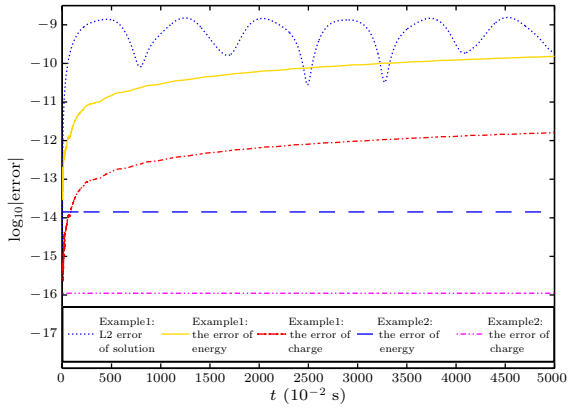

Fig. 3. The absolute error of solution and the discrete conservation error of energy and charge within 50 s.

Then we consider example 2 with the initial condi-

tion $\varphi(x) = \frac{\sqrt{2K}}{\cosh(\sqrt{2K}x)}$ and suppose $\alpha = \frac{1}{2}$, $\gamma = 1$ and $\beta = -\frac{1}{2}$, where K is the eigenvalue of the nonlinear eigenvalue problem $KP = \frac{1}{2}P + |P|^2P - \frac{1}{2}P$. Figure 2 shows that, with the augment of eigenvalue, the amplitude becomes greater and the beam width narrows down until the appearance of peakons. Hence, one can select an appropriate K to ensure the stationary waves broaden in a predictable way. As shown in Fig. 3, the proposed scheme is able to simulate the wave of example 1 very well within 50 s, and the global energy and charge invariants are also preserved well, which are in accordance with Eqs. (2) and (3).

For example 3, we suppose that $\alpha = \frac{1}{2}\cos(t)$, $\gamma = \frac{\cos(t)}{\sin(t)+3}$, $\beta = 0$ with the initial condition $\varphi(x) = \frac{1}{\sqrt{3}}\mathrm{sech}(\frac{x}{3})\exp(\frac{i(x^2-1)}{6})$. Consequently, the plot in Fig. 4(a) displays the periodic behavior almost perfectly, and the amplitude of $|\Psi|^2$ shows a cyclic change. According to the perturbation theory of quantum mechanics, we take the first order distorted approximation, namely $\alpha = \frac{1}{2}(\cos(t) + \sqrt{2}\cos(\sqrt{2}t))$, $\gamma = \frac{\cos(t)+\sqrt{2}\cos(\sqrt{2}t)}{\sin(t)+\sin(\sqrt{2}t)+5}$. Then we obtain the quasi-periodic solution whose peak value of density causes any distortion with time. Furthermore, Fig. 5 shows the central-peak value of the waveform (Figs. 5(a) and 5(b)) within 50 s. As seen from Fig. 5(c), the charge is also preserved well.

Table 1. Computing error of two different schemes.

L_∞	10 s	30 s	40 s	50 s
CFDM	2.4103×10^{-13}	3.4006×10^{-13}	4.7909×10^{-13}	5.1903×10^{-13}
FPSM	1.7764×10^{-13}	1.8874×10^{-13}	5.1559×10^{-12}	1.5951×10^{-12}

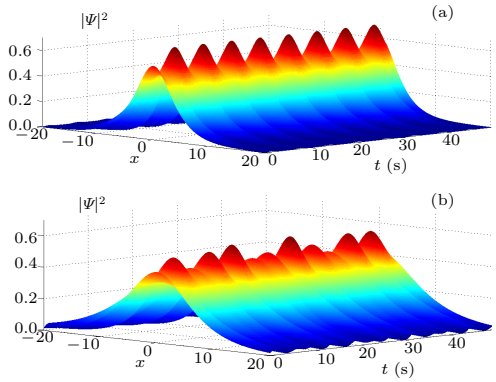

Fig. 4. Periodic solitary wave and quasi-periodic wave with the harmonic trap potential ($L = 20$, $N = 400$ and $dt = 0.005$) on one single period interval.

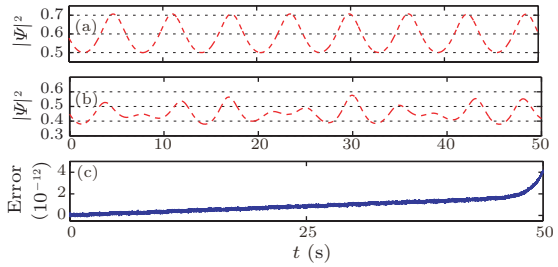

Fig. 5. Example 3: the peak values of condensate density within 50 s: (a) periodic solitary wave, (b) quasi-periodic wave, and (c) the discrete conservation error of charge for periodic solitary wave.

Additionally, Eq. (1) has a bright solitary wave with the harmonic trap potential $X = \frac{1}{2}x^2$ under the homogeneous boundary condition. This solution usually serves as a relatively accurate and simple model of a parabolic trap in example 4. Here we let $\alpha = \frac{1}{2}$, $\gamma = 1 + \gamma_0\sin(t)$, $\beta = -\frac{\cos^2(t)+10\sin(t)+1}{2(10+\sin(t))^2}$, and take the initial condition with $\varphi(x) = f_0\mathrm{sech}(x)\exp(i(x - \frac{1}{10}x^2))$. The intensity $|\Psi|^2$ displays periodic oscillations plotted on Fig. 6 for the reason that the external potential function changes from attractive to repulsive, and the amplitude of fluctuation becomes larger with spreading far away from the restrictions of the initial condition. As is expected, we observe that the velocity of the pulse center increases periodically and the numerical solution conserves very well the discrete charge invariant as illustrated in Fig. 7.

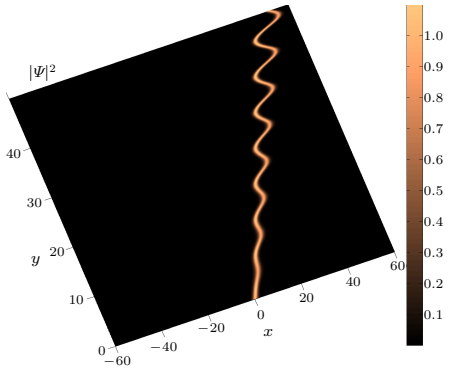

Fig. 6. The bright solitary (BS) solution with the harmonic trap potential ($L = 60$, $N = 600$, $dt = 0.005$, $\gamma_0 = f_0 = 0.1$).

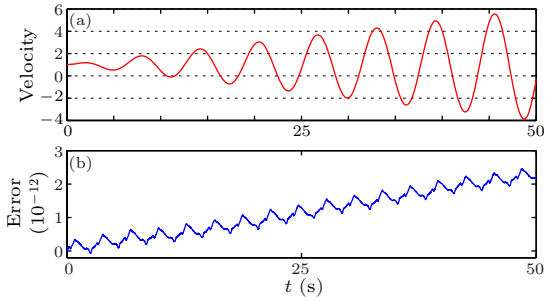

Fig. 7. Example 4: the velocity of the waveform center pulse and the discrete conservation error of charge.

In summary, we have proposed a scheme combined with CFDM and AVFM to describe various waveforms in BEC containing time-dependent coefficients in some small potentials. Numerical results show that the new

high order method finely depicts some kinds of condensate wave density and preserves the charge within slight error. In addition, the energy conservation law is also conserved under specific conditions. Finally, the comparison with the FPSM method verifies that the proposed method is robust and suitable for more numerical experiments of long time simulation.

References

[1] Kunze M 1999 *Physica* D **128** 273
[2] Kivshar Y S, Alexander T J and Turitsyn S K 2001 *Phys. Lett.* A **278** 225
[3] Mallory K and Van Gorder R A 2014 *Phys. Rev.* E **89** 013204
[4] Hong J L and Kong L H 2010 *Commun. Comput. Phys.* **7** 613
[5] Bao W Z and Shen J 2005 *SIAM J. Sci. Comput.* **26** 2010
[6] Dehghan M and Taleei A 2010 *Comput. Phys. Commun.* **181** 43
[7] Zhou X F, Zhang S L, Zhou Z W, Malomed B A and Pu H 2012 *Phys. Rev.* A **85** 023603
[8] Cartarius H and Wunner G 2012 *Phys. Rev.* A **86** 013612
[9] D Agosta R and Presilla C 2002 *Phys. Rev.* A **65** 043609
[10] Bronski J C, Carr L D, Deconinck B, Kutz J N and Promislow K 2001 *Phys. Rev.* E **63** 036612
[11] Chen Y M, Song S H and Zhu H J 2012 *Appl. Math. Comput.* **218** 5552
[12] Lv Z Q, Wang Y S and Song Y Z 2013 *Chin. Phys. Lett.* **30** 030201
[13] Qian X, Fu H and Song S H 2016 *Appl. Math. Comput.* **307** 1
[14] Hu W P, Deng Z and Yin T 2017 *Commun. Nonlinear. Sci.* **42** 298
[15] Ma Y P, Kong L H and Hong J L 2011 *Comput. Math. Appl.* **61** 319
[16] Qian X, Song S H, Gao E and Li W B 2012 *Chin. Phys.* B **21** 070206
[17] Cai J X and Wang Y S 2013 *Chin. Phys.* B **22** 060207
[18] Quispel G R W and McLaren D I 2008 *J. Phys.* A **41** 045206
[19] Celledoni E, Grimm V, McLachlan R I, McLaren D, O Neale D, Owren B and Quispel G 2012 *J. Comput. Phys.* **231** 6770
[20] Zhang H, Song S H, Chen X D and Zhou W E 2014 *Chin. Phys.* B **23** 070208
[21] Jiang C L and Sun J Q 2014 *Chin. Phys.* B **23** 050202
[22] Cai J X, Wang Y and Gong Y 2015 *J. Sci. Comput.* **1** 36